Brain Imaging and Behavior
https://doi.org/10.1007/s11682-020-00395-3

ORIGINAL RESEARCH

Intrinsic non-hub connectivity predicts human inter-temporal decision-making

Qiang Wang[1,2,3] · Yuxuan Zhu[2] · Yajie Wang[2] · Chuansheng Chen[4] · Qinghua He[5,6] · Gui Xue[7]

Accepted: 2 September 2020

Abstract

Inter-temporal decision-making is ubiquitous in daily life and has been considered as a critical characteristic associated with an individual's success. Such decisions require us to tradeoff between short-term and long-term benefits. Prior studies have indicated that inter-temporal decision involves various brain regions that tend to occupy the central hubs. However, it is unclear whether the functional connectivities among hub as well as non-hub regions can predict discounting behaviors. Here, we combined with graph-theoretical algorithm and multivariate pattern analysis to explore whether voxel-wise functional connectivity strength in the whole brain could predict discounting rates (indexed as *logk*, based on the adaptive delay-discounting task) in a relatively large sample ($n = 429$) of young adults. Results revealed that short- and long-distance as well as all-range non-hub functional connectivity strength in the limbic system (i.e., medial orbitofrontal cortex and parahippocampus) were inversely associated with discounting rates. Furthermore, these results were robust and did not appear to be due to potential confounding factors. Above weight-based degree metric is commonly indicative of the communication pattern of local and global parallel information processing, and it therefore provides novel insights into the neural mechanisms underlying inter-temporal decision-making from the perspective of human brain topological organizations.

Keywords Inter-temporal decision-making · Multivariate pattern analysis · Functional connectivity strength · Hub region

Introduction

Inter-temporal decision-making has been considered as a critical characteristic associated with an individual's success. In such choices, people are more likely to prefer immediate outcomes rather than future outcomes, which is also called delay-discounting phenomenon (Bickel et al. 1999; McClure et al. 2004). Steep delay discounting behavior was often observed in substantial psychiatric disorders such as substance abuse (Bickel et al. 1999; Hu et al. 2015), pathological gambling (Alessi and Petry 2003), and attention deficit hyperactivity disorder (ADHD) (Paloyelis et al. 2010).

Electronic supplementary material The online version of this article (https://doi.org/10.1007/s11682-020-00395-3) contains supplementary material, which is available to authorized users.

✉ Qinghua He
heqinghua@swu.edu.cn

✉ Gui Xue
gxue@bnu.edu.cn

[1] Key Research Base of Humanities and Social Sciences of the Ministry of Education, Academy of Psychology and Behavior, Tianjin Normal University, Tianjin 300387, China

[2] Faculty of Psychology, Tianjin Normal University, Tianjin 300387, China

[3] Tianjin Social Science Laboratory of Students' Mental Development and Learning, Tianjin 300387, China

[4] Department of Psychological Science, University of California, Irvine, CA 92697-7085, USA

[5] Faculty of Psychology, Southwest University, Chongqing 400715, China

[6] CAS Key Laboratory of Mental Health, Institute of Psychology, Beijing 100101, China

[7] National Key Laboratory of Cognitive Neuroscience and Learning, IDG/McGovern Institute for Brain Research, Beijing Normal University, Beijing 100875, China

Published online: 10 October 2020

Accumulated evidence has consistently implicated that inter-temporal decision-making did not depend on any isolated brain regions but several functional networks and their communication/integration between them. Such networks have been reliably summarized as the valuation network (i.e., ventral striatum [VS], ventromedial prefrontal cortex [VMPFC], and posterior cingulate cortex [PCC]), cognitive control network (i.e., dorsolateral prefrontal cortex [dlPFC], and superior parietal lobule [SPL]), and prospection network (i.e., hippocampus, parahippocampus, and medial orbitofrontal cortex [mOFC]) (Berns et al. 2007; Lempert and Phelps 2016; Peters and Büchel 2011). Furthermore, connectome-based analyses consistently highlighted the importance of network-based interaction (i.e., fronto-parietal network, default mode network, and salience network) instead of regional dynamics (Chen et al. 2017; Li et al. 2013; van den Bos et al. 2014; Van Den Bos et al. 2015a) in the inter-temporal decisions. In addition, the neuroanatomical evidence has also identified a series of structural subnetworks associated with discounting behaviors, including the valuation network (i.e., VS and VMPFC) and prospection network (i.e., hippocampus and parahippocampus) (Dombrovski et al. 2012; Yu 2012). Taken together, network-based analytical framework is a critical step to explore the mechanisms underlying the inter-temporal decisions, but the extent to what the global and local information communications and integrations of voxel-wise whole-brain network support human inter-temporal decision-making is still not clear.

Using graph-theoretical algorithms and multi-modal neuroimaging data, prior studies have examined the possible relationships between delay-discounting and multiple topological metrics of human brain connectomes, including the small-world organization, network efficiency, modularity dynamic, hierarchical structure, cardinal nodal attributes in degree and betweenness centrality in both functional and structural brain networks (Cai et al. 2020; Chen et al. 2019b; Li et al. 2013). Some of them revealed decreased global topological organizations including small-world property and rich-club regimes in both functional and structural brain networks, and also observed the dreadful local topological dynamics in the modularity of functional connectome in the participants with steep discounting rates (Chen et al. 2019b). Others indicate that the discounting rates could be successfully predicted by functional connectivity intensity, namely nodal degree, within and between several sub-networks via linear prediction model (Cai et al. 2020; Li et al. 2013). Such nodal degree is widely used to quantify nodal properties and importance in a graph, and is defined as the number of connections that link it to the rest of the network (Bondy and Murty 1976; Bullmore and Sporns 2009). Moreover, **the cortex contains a small number of nodes, referred to as hubs that have disproportionately numerous connections (**Sporns et al. 2007**). Such hubs in functional networks were reported in several areas, including the default-mode network and executive control network that commonly were involved to inter-temporal decisions (**Oldham and Fornito 2019**;** van den Heuvel and Sporns 2013**), and are thought to be crucial to efficient communication between separated and long-distance regions** (Bullmore and Sporns 2009; Freeman et al. 1991). However, to our knowledge, no study has systematically investigated whether delay-discounting rates could be predicted by the topological metrics in these hub regions, especially from a voxel-wise whole-brain approach, which overcomes the drawbacks of parcellation-based degree computation (de Reus and Van den Heuvel 2013).

Multi-voxel pattern analysis (MVPA) approach has widely been applied in human brain imaging studies and led to fundamental advances in the understanding of how the brain represents information as well as is particularly suitable for probing subtle and spatially distributed differences between separated cognitive states (Haxby 2012; Haxby et al. 2014; Norman et al. 2006). In decades, this approach was widely used to distinguish category-dependent and category-independent goal value codes (McNamee et al. 2013), classify different types of valuation (Clithero et al. 2009), decode gain and loss processing (Jimura and Poldrack 2012), and predict the following choices (Zha et al. 2019) and individual's behavioral performances (Wang et al. 2016) in the decision-making domain. Furthermore, MVPA is more sensitive to distributed coding of information compared to univariate analysis (Jimura and Poldrack 2012; Wang et al. 2014a). Although the advantages of MVPA have been ascertained in the domains of decision-making, its corresponding insights into inter-temporal decision-making are still poorly unknown.

In the current study, we collected resting state fMRI data and assessed everyone's delay-discounting parameter using an adaptive delay-discounting task in a relatively large sample ($n = 429$) of young adults. Using a voxel-wise whole-brain connectivity analysis approach and MVPA, we comprehensively examined the potential contributions of the network nodal connectivity capacity to individual variability in inter-temporal decision-making.

Methods and materials

Participants

Four hundred and twenty-nine (315 females and 114 males) healthy Chinese college students were recruited in this study (age ranged from 17 to 26 years old, with mean age = 19.58 ± 1.59 years). Subjects were included if they had high-quality structural and functional imaging data, with small head motion during fMRI scan (***frame-wise displacement [FD]*** < 1 mm), and good model-fitted behavioral scores (k) based on previous studies (Wang et al. 2016). All subjects reported no history of psychiatric or neurological disease. Written informed consent was obtained for each adult participant (age 18–26) before the experiment. Four adolescent participants (age 17) were required to sign the consent form after receiving the verbal consent from their parents. The Institutional Review Boards of Southwest University and Beijing Normal University approved this study.

Adaptive delay discounting task

The adaptive delay-discounting task was used to measure delay-discounting rate (See previous study for details, van den Bos et al. 2014). In brief, subjects were asked to make a decision between a fixed but immediate monetary option (SS)(RMB ¥60) and a varied delayed but larger monetary option (LL)(RMB ¥78–108 to be paid in 15 to 45 days later). The size of the delayed reward was adjusted to converge toward the same subjective value as the immediate option (RMB ¥60). We used a hyperbolic function ($SV = A/(1 + k*D)$) to calculate individual's delay-discounting rate, where SV is the subjective value of the LL option, A is the magnitude in Chinese dollars of the delayed reward, D is the delay time, and k is the delay-discounting rate. Initial discounting rate k was set to 0.02 and was increased or decreased when the subjects chose the immediate or delayed option, respectively. Based on past literature (Johnson and Bickel 2002), hypothetical money served as a valid proxy for real money. In addition, all participants received monetary compensation of RMB 500 at the end of our experiments.

Behavioral data analysis

All behavioral and statistical analyses were conducted using MATLAB (MathWorks, Natick, MA, USA). In the discounting task, we used the multidimensional unconstrained nonlinear minimization function (*fminsearch*) of the optimization toolbox implemented in MATLAB to calculate everyone's magnitude of delay-discounting rate (*k*). In this process, the softmax function was utilized to calculate the probability of choosing the immediate option (P_{SS}) on trial t as a function of the difference in V_{SS} and V_{LL}: $P_{SS} = 1/(1 + \exp.(-1*m*(V_{SS}-V_{LL})))$, where m is the decision slope, V_{SS} and V_{LL} are the subjective values of SS and LL options, respectively. Individual discounting rates were determined as the value k that maximized the likelihood of the observed choices. We further used log-transformed k to represent decision impulsivity (log*k*) based on prior research (Van Den Bos et al. 2015b; Wang et al. 2016).

Brain imaging data acquisition

All structural and resting-state functional MRI images were acquired on a Siemens 3 T Trio scanner (Siemens Medical Systems, Erlangen, Germany). High-resolution T1-weighted structural images were acquired by using a Magnetization Prepared Rapid Acquisition Gradient-Echo (MPRAGE) sequence: TR/TE = 1900 ms/2.52 ms; inversion time (TI) = 900 ms; flip angle = 9 degree; FOV = 256 × 256 mm^2; Slice = 176; thickness = 1.0 mm; voxel size = 1 × 1 × 1 mm^3. Functional MRI images were collected based on the Gradient Echo type Echo Planar Imaging (GRE-EPI) sequence; TR/TE = 2000 ms/30 ms; Flip angle = 90 degree; Resolution matrix = 64 × 64; FOV = 220 × 220 mm^2; Thickness = 3 mm; slip gap = 1 mm; acquisition voxel size = 3.4 × 3.4 × 4 mm^3. A total of 32 slices were employed to cover the whole brain. Each section contained 242 volumes. During the resting-state scanning, all subjects were required to relax and keep their eyes closed but not to sleep (Damoiseaux et al. 2006).

Resting-state fMRI preprocessing

The resting-state fMRI data were preprocessed using Data Processing Assistant for Resting-State fMRI (DPARSF, http://resting-fmri.sourceforge.net/) implemented in the MATLAB (Math Works, Natick, MA, USA) platform. The first 10 volumes of each participant were discarded due to the magnetization disequilibrium and the subject's adaptation to the scanning noise. The remaining 232 volumes were slice-timing corrected and then realigned to the middle slice of the brain to correct for head motion. All realigned images were spatially normalized to the MNI template, resampled into 3 × 3 × 3 mm^3 resolution. White matter, cerebrospinal fluid, global signal, and six motion parameters for head movement were regressed out as nuisance variables to reduce the effects of head motion and non-neuronal BOLD fluctuations (Fox et al. 2005). Temporal filtering (0.01–0.08 Hz) and voxel-wise linear detrending were also applied to the resting-state fMRI data (Shin et al. 2014). It should be noted that the strategy of smoothing was not conducted in this study because the multivariate pattern analysis.

Voxel-wise network nodal connectivity measurements

To assess network nodal connectivity, we first calculated Pearson's correlations between the time series of all pairs of voxels within a predefined gray matter mask with 45,892 voxels by aligning probability SPM gray matter mask (gray matter probability values higher than 0.2) to atlas space, which yielded a whole-brain functional connectivity matrix. Then, we transformed the individual correlation matrices to z-score matrices using a Fisher's *r*-to-*z* transformation to improve the normality of the correlation matrices. Third, a threshold (here is $r = 0.2$, the threshold effects were estimated in the "Validation Analysis") was chosen to eliminate the effects of signal noise from weak or negative correlations. Finally, for each voxel, we calculated its functional connectivity strength (FCS) as the sum of the weights (*z*-values) of the connections between a given voxel and all of the other voxels. Notably, the FCS matric reflects the "degree centrality" of the weighted networks in terms of graph-theory and captures the global communication ability of brain regions in the whole networks (Liang et al. 2013).

Support vector regression (SVR) analysis

The preprocessed FCS data without smoothing were employed to predict individual k using Epsilon-intensitive support vector regression (SVR) (Drucker et al. 1997) implemented in PyMVPA (Multivariate Pattern Analysis in Python: http://www.pymvpa.org/). **The linear kernel was used in this study due to high generalization and interpretation (**Cox and Savoy 2003**;** Norman et al. 2006**)**. A searchlight procedure with ***a three-voxel radius (9 mm) sphere*** (Kriegeskorte et al. 2006) was utilized to produce the decoding accuracy in the neighborhood of each voxel. Following the previous literature (He et al. 2013; Jimura and Poldrack 2012; Wang et al. 2016), we set the ε parameter in the SVR to be 0.01.

A ten-fold cross-validation was applied. The 429 subjects were divided into 10 groups of 42 or 43 subjects, with matched gender as well as matched log*k*, depending on the specific analysis. We firstly regressed out the confounding variables such as gender and age from the whole sample. Then, an SVR model was trained based on 386 or 387 subjects. Once trained, this SVR model then generated a prediction from the scores of the excluded 42 or 43 subjects based on their imaging data. Voxel-wise accuracy of SVR prediction was then calculated as the Pearson's correlation coefficient between actual and predicted values of the log*k* and then transformed to the corresponding Z-score map. Multiple comparisons were corrected at the cluster level for each analysis ($z > 3.1$, $p < 0.001$, family-wise error (FWE) corrected $p < 0.05$)(Eklund et al. 2016).

Univariate analysis

To further explore the correlations between nodal functional connectivity and behavioral delay-discounting rate (*logk*), we selected the significantly predicted brain areas as the regions of interest (ROIs), including the left parahippocampus (lPHG), hippocampus (HIP), medial orbitofrontal cortex (mOFC), and frontal pole (FP), because these brain regions frequently are observed involved into inter-termporal decision-making in considerable studies (Peters and Büchel 2011). Then, we extracted these ROIs' average functional connectivity strengths and correlated them with behavioral discounting rate (*logk*). Due to the double dipping issues, we only presented the correlational directions without reporting the correlation coefficients.

Next, to investigate whether the brain regions related to delay-discounting occupied the brain hub regions or not, we used two strategies. First, for each subject, we computed the mean FCS within the discounting-related brain areas and the mean FCS of the remaining areas. We then used paired-sample t-tests to determine whether the impulsivity-related regions had higher FCS than all of the other regions. Second, to directly estimate whether the discounting-related brain regions were brain hubs, we first computed a group-level FCS maps by averaging each individual's FCS maps, and then defined the brain network hubs by identifying voxels with the FCS values of 1 SD above the mean based on prior studies (Liu et al. 2017). Then, we calculated the hub proportion, P_{hub}, which is the proportion of discounting-related regions belonging to brain hubs.

Finally, to further examine the effects of anatomical distance on connectivity analysis, we divided the regional functional connectivity strength into two categories, short-distance and long-distance regional functional connectivity strength. The short-distance regional functional connectivity strength of a voxel referred to the sum of those connections (Z-values) between the voxel and other GM voxels with anatomical distances less than 75 mm to the given voxel, whereas the long-distance regional functional connectivity strength of a voxel referred to the sum of its connections (Z-values) with distances greater than 75 mm (Achard et al. 2006; He et al. 2007; Wang et al. 2014b). In this study, the anatomical distance between two GM voxels was calculated based on the Euclidean distance between their MNI coordinates. Hence, we can further investigate whether distance-dependent FCS can also predict decision impulsivity.

Controlling for potential confounding factors

To validate our major findings, we examined how potential confounding factors might have influenced the experimental results. First, considering the skewed distribution of behavioral *logk*, we conducted a rank-based inverse Gaussian transformation (Beasley et al. 2009) and further examined the prediction of FCS on this transformation-based delay-discounting rate. Second, due to the phenomenon that head motion has an adverse influence on functional connectivity-related analyses, we regressed out the effect of head motion and then performed MVPA again. Third, global signals have been considered another factor that influences the network-related statistical analyses and thus we repeated our network analysis without global signal regression. Fourth, to determine whether the major results depend upon the selection of correlation thresholds for connectivity, we recomputed the FCS maps using different correlation thresholds (i.e., 0.1, 0.3 and 0.4) and then re-performed MVPA. Finally, we evaluated whether the smoothing process would change the major results in light of the fact that the smoothing process reduces the signals of brain in MVPA and then re-performed the MVPA with a Gaussian kernel with a full width half maximum of 4 mm.

Results

Behavioral results

The mean discounting rate (*logk*) was −1.96 ± 0.49, ranging from −3.64 to −0.75. Figure 1a depicts the distribution of discounting rates in whole sample, which manifested skewed (Kolmogorov-Smirnov test, $p < 0.001$). The mean head motion (FD) was 0.108 ± 0.044, ranging from 0.043 to 0.255. There was no significant correlation between the discounting rates and head motion ($r = -0.025$, $p = 0.605$), which suggests that head motion should have had little impact on subsequent analyses. Additionally, gender differences were also not detected in impulsivity ($t_{(427)} = 1.20$, $p = 0.231$).

Network nodal connectivity associated with delay-discounting rate

The voxel-wise multivariate analysis revealed that individuals' k could be successfully predicted by the FCS values, primarily those from the right medial orbitofrontal cortex (mOFC; MNI = 24, 18, −18, Z = 5.31), left parahippocampus gyrus (PHG; MNI = −24, −2, −36; Z = 4.66), left precuneus (MNI = −18, −66, 34, Z = 4.68), right lateral orbitofrontal cortex (LOFC; MNI = 40, 40, −18, Z = 4.19), left putamen (MNI = −30, −6, −6; Z = 4.65), right frontal pole (FP; MNI = 12, 64, −12, Z = 3.79), left temporal fusiform cortex (TFC; MNI = −36, −24, −24, Z = 3.80), right occipital pole (MNI = 24, −94, 0; Z = 4.83), and right hippocampus (MNI = 26, −20, −12, Z = 3.63) (Fig. 1b **and** Table 1).

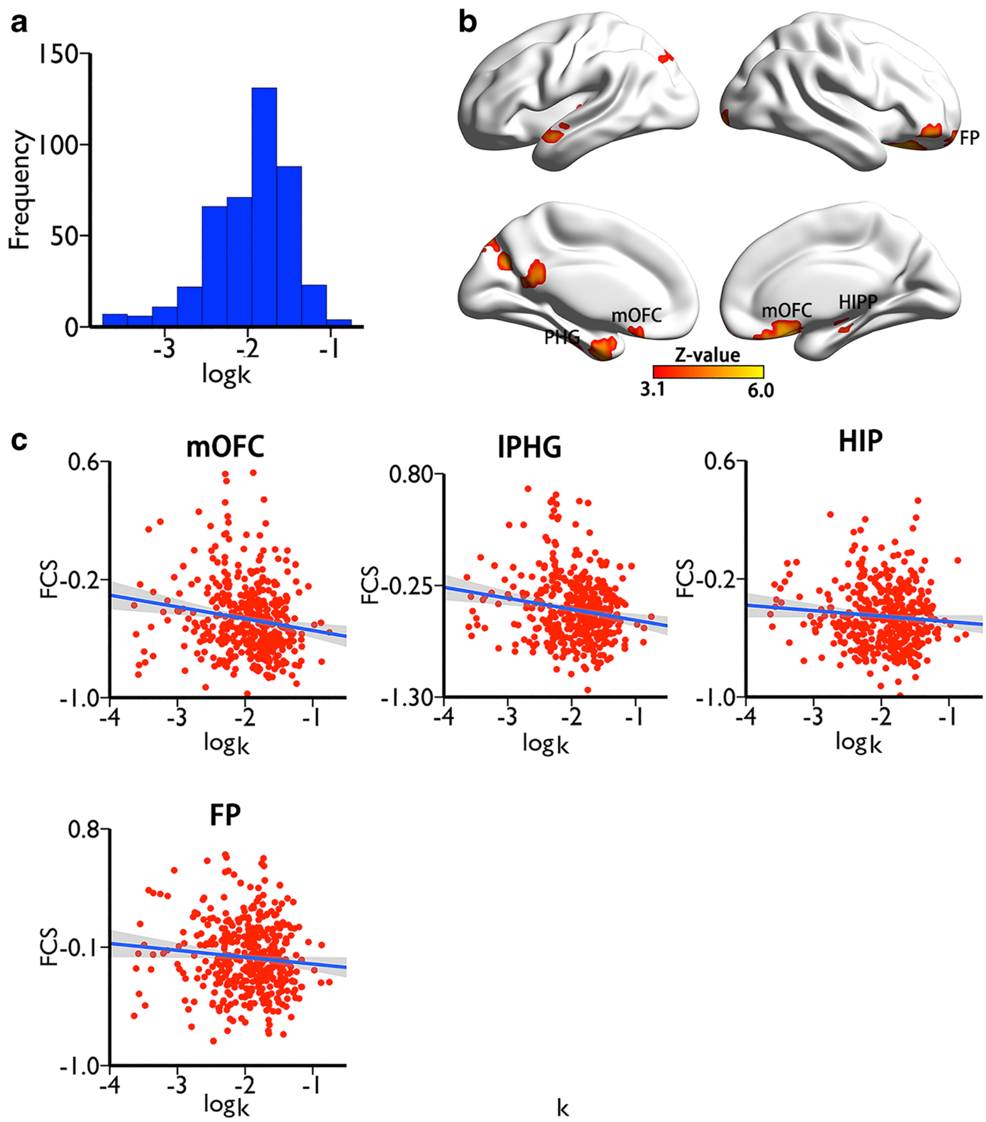

Fig. 1 The distribution of individuals' delay-discounting rates (log*k*) and the brain regions whose FCS predicted discounting behaviors. (a) The distribution of the discounting rates was skewed (Kolmogorov-Smirnov test, $p < 0.001$). (b) MVPA revealed that the FCS values in these regions could predict decision impulsivity ($z > 3.1$, FWE corrected $p < 0.05$). (c) Scatter plots show correlations between discounting rates and the FCS of the sphere clusters with 3 mm radius based on the peak in mOFC, HIPP, lPHG, and FP. Abbreviation: HIP, hippocampus; mOFC, medial orbitofrontal cortex; lPHG, left parahippocampus gyrus; FP, frontal pole

Table 1 Brain regions whose FCS predicted delay-discounting rates across different ranges in multivariate analysis

Brain regions	*L/R*	*No. Voxels*	*MNI Coordinates*			*Z*
			X	*Y*	*Z*	
All-range FCS						
Medial OFC	R	745	24	18	−18	5.31
Parahippocampus gyrus	L	259	−24	−2	−36	4.66
Precuneus	L	119	−18	−66	34	4.68
Lateral OFC	R	93	40	40	−18	4.19
Putamen	L	85	−30	−6	−6	4.65
Frontal Pole	R	69	12	64	−12	3.79
Temporal fusiform cortex	L	58	−36	−24	−24	3.80
Occipital pole	R	35	24	−94	0	4.83
Hippocampus	R	15	26	−20	−12	3.63
Short-distance FCS						
Medial OFC	R	175	24	18	−20	4.11
Temporal Pole	L	162	−24	4	−28	4.32
Lateral occipital cortex	L	162	−26	−74	34	4.67
Middle temporal gyrus	L	96	−64	−42	−12	4.85
Supramarginal gyrus	R	86	66	−40	18	4.90
Frontal Pole	L	80	−48	38	14	4.82
Temporal pole	R	78	46	12	−24	4.23
Lateral occipital cortex	R	70	34	−58	42	5.00
Thalamus	R	67	18	−18	12	4.69
Parahippocampus	R	61	22	−10	−28	3.95
Temporal pole	R	55	60	6	−30	4.15
Frontal Pole	R	33	52	42	4	4.09
Lateral OFC	R	32	42	40	−18	4.30
Long-distance FCS						
Precuneus	–	576	0	−60	18	4.92
Medial OFC	R	143	16	24	−18	4.19
DMPFC	L	36	−12	30	36	4.21
Parahippocampus	R	36	24	−24	−18	4.05
Parahippocampus	L	27	−30	0	−26	3.73
Lateral occipital cortex	L	23	−30	−70	34	3.63
Lateral OFC	R	23	24	28	−16	3.94
Insular	L	23	−36	12	−2	3.63
Inferior Frontal gyrus	L	22	−50	30	18	4.02

Abbreviation: OFC, orbitofrontal cortex; DMPFC, dorsal medial prefrontal cortex; L, left; R, right

Furthermore, the correlational analysis revealed that, the FCS values in these brain regions that are widely demonstrated involved into inter-temporal decisions (i.e., mOFC, left PHG, hippocampus, and FP) were negatively associated with decision impulsivity (Fig. 1c).

To rule out the possibility of the impact of the skewed behavioral distribution on the findings, we used a rank-based inverse Gaussian transformation method to transform the behavioral scores and re-performed the multivariate pattern analysis. **Fig. S1** displays the main results, which substantiated that behavioral distribution did not change the major findings. Moreover, when controlling additionally for gender and age, these results still remained significant (**Fig. S1**). In sum, our main findings were not confounded by biased gender ratio, skewed behavioral distribution, or subjects' age.

Engagement of the non-hub functional networks in inter-temporal decision-making

The brain regions related to delay-discounting were predominantly located in the non-hub areas, as shown by the discounting-related regions' lower FCS values than those of the other regions ($t_{(428)} = -13.30$, $p = 4.90 \times 10^{-34}$) (Fig. 2a). A stringent FCS threshold based on previous studies (Liu et al. 2017) (i.e., above 1 SD of the mean FCS) led to the identification of areas predominantly distributed in the PCC/PCU, the medial prefrontal cortex (MPFC), the lateral frontal and parietal cortices (Fig. 2b), which was largely consistent with previous studies (Buckner et al. 2009). A further analysis revealed that the overlap between the discounting-related regions and the hub regions was small (3.1%, black color, Fig. 2b). Taken together, these findings indicated that non-hub nodal capacity plays a critical role in inter-temporal decision-making.

Connectivity distance and the relation between FCS and decision impulsivity

For short-distance functional connectivity strength, individuals' log*k* could be successfully predicted by the FCS values in the right mOFC (MNI = 24, 18, −20, Z = 4.11), right parahippocampus (MNI = 22, −10, −28, Z = 3.95), right lateral OFC (MNI = 42, 40, −18, Z = 4.30), left temporal pole (MNI = −24, 4, −28, Z = 4.32), left LOC (MNI = −26, −74, 34, Z = 4.67), right LOC (MNI = 34, −58, 42, Z = 5), left middle temporal gyrus (MNI = −64, −42, −12, Z = 4.85), right supramarginal gyrus (SMG; MNI = 66, −40, 18, Z = 4.90), left FP (MNI = −48, 38, 14, Z = 4.82), right FP (MNI = 52, 42, 4, Z = 4.09), right temporal pole (MNI = 46, 12, −24, Z = 4.23), right LOC (MNI = 34, −58, 42, Z = 5.00), and right thalamus (MNI = 18, −18, 12, Z = 4.69) (Fig. 3a **and** Table 1).

For long-distance functional connectivity strength, individuals' k could be predicted by the FCS values in several brain areas, including the left dorsomedial prefrontal cortex (DMPFC; MNI = −12, 30, 36, Z = 4.21), precuneus/PCC (MNI = 0, −60, 18, Z = 4.92), right mOFC (MNI = 16, 24, −18, Z = 4.19), right lateral OFC (MNI = 24, 28, −16, Z = 3.94), right parahippocampus (MNI = 24, −24, −18, Z = 4.05), left parahippocampus (MNI = −30, 0, −26, Z = 3.73), left LOC (MNI = −30, −70, 34, Z = 3.63), left inferior frontal

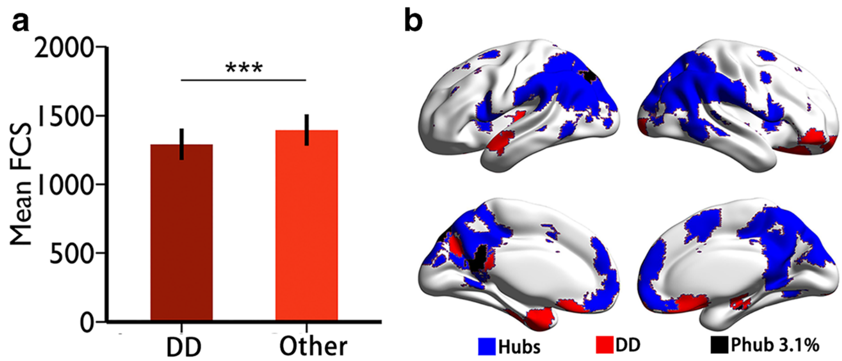

Fig. 2 Non-hub functional network in relation to inter-temporal decision-making. (a) The bar map shows that the mean FCS value (Z-score) within the significant regions that predicted delay-discounting (DD) was smaller than that of other regions. The error bar represents SD, *** $p < 0.001$. (b) The overlapping maps between the regions that predicted DD and the network hubs (above 1 SD beyond the mean). Blue indicates the hub areas, and red indicates impulsivity-related regions. The overlapping regions (3.1%, Phub) are presented as black patches

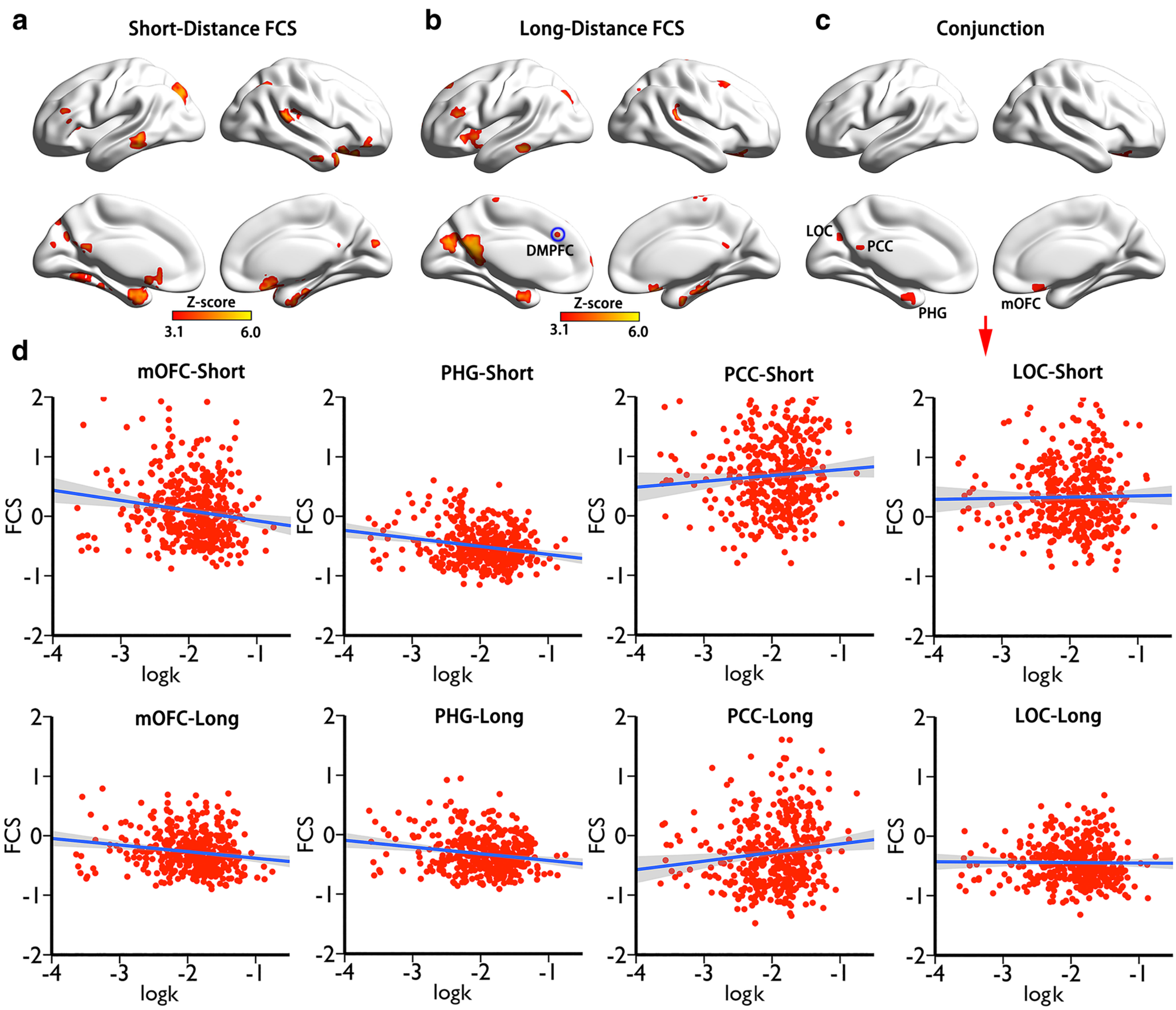

Fig. 3 The relationships between the short/long-distance FCS and inter-temporal decision-making. (a) and (b) respectively indicates the regions that predicted the discounting rates using MVPA ($z > 3.1$, FWE corrected $p < 0.05$). (c) shows the conjunction regions that predicted discounting behaviors among all-range, long-distance and long-distance FCS analysis. (d) Scatter plots display the prediction directions between the nodal FCS in the conjunction analysis and discounting behaviors in short- and long-distance FCS conditions. DMPFC, dorsal medial prefrontal cortex; FCS, functional connectivity strength

gyrus (IFG; MNI = −50, 30, 18, Z = 4.02), and left insula (MNI -36, 12, −2, Z = 3.63) (Fig. 3b **and** Table 1).

A conjunction analysis of all-range, short-distance, and long-distance FCS revealed that log*k* could be predicted by the FCS values in several common regions, including mOFC, parahippocampus, PCC, and LOC (Fig. 3c). The correlational analysis suggested that the FCS in mOFC and parahippocampus were inversely associated with decision impulsivity regardless of the functional connectivity distance, while both short- and long-distance FCS in PCC and short-distance FCS in LOC were positively associated with decision impulsivity (Fig. 3d).

Consideration of additional potential confounding factors

We assessed the reproducibility of our major results after considering different potential confounding factors such as head motion, global signal, correlation threshold, and smoothing process. The results remained consistent under these factors, as indicated by the high frequency of the spatial overlap of the impulsivity-related regions among validations (Fig. 4).

Discussion

This study utilized a multivariate pattern analysis approach and graph-theoretical algorithms to investigate whether FCS can predict delay-discounting rate in a relatively large sample. Our results indicated that short- and long-distance as well as all-range non-hub FCS in the limbic system (i.e., mOFC and parahippocampus) could successfully predict discounting rates. These results were robust and did not appear to be due to potential confounding factors. Our findings indicated an intrinsic functional network organization underlying the individual variability in inter-temporal decision-making, and the brain non-hub regions play an indispensable role in network organization and communication related to impulsivity.

In human connectomes, the degree was proven to be the most pivotal nodal measures to quantitatively delineate the position of nodes within the networks, reflecting the capability of brain regions on parallel information processes (Hagmann et al. 2008; Sporns 2011). Previous studies have demonstrated close spatial couplings between functional brain regions with higher degree, indexed as FCS, and regional cerebral blood flow in both resting-state and task demands, suggesting the physiological basis of blood supply for brain functional topological metrics especially for FCS (Liang et al. 2013). In recent years, this metric has widely used to bridge between brain global communication/functional integration and numerous cognitive processes, including spatial working memory (Liu et al. 2017), language (Zhang et al. 2018), executive function(Zhang et al. 2018), and even psychiatric disorders such as Alzheimer's disease (Franzmeier et al. 2018). Collectively, the FCS might be a sensitive index to capture human brain topological organization and corresponding associations with cognitive and behavioral performances. Encouragingly, the present study likewise observed such associations of delay-discounting behavior with brain topological metric of FCS in several brain regions, including frontal pole, hippocampus, parahippocampus, and medial OFC.

The brain areas mentioned above have been frequently demonstrated engaged to inter-temporal decision-making in both functional and structural MRI studies. More specially, the frontal pole (FP) is a part of the prefrontal cortex and approximately corresponds to Brodmann's area 10 (Öngür et al. 2003; Ramnani and Owen 2004). There is mounting evidence that FP predominantly involves in many higher-

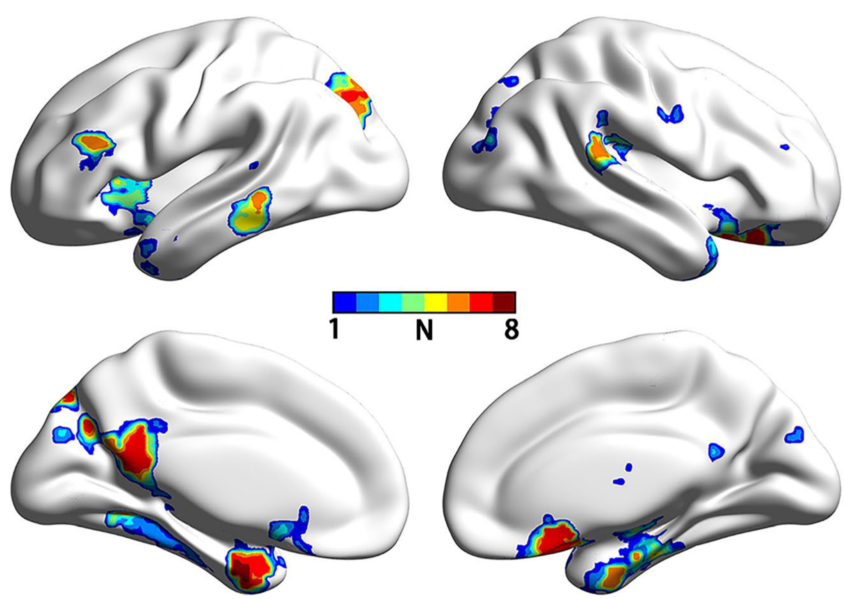

Fig. 4 Conjunction map after controlling for potential confounding factors. The brain map shows the frequencies of the spatial overlap of the impulsivity-related regions identified by eight different image preprocessing and data analysis strategies. The regions with higher frequencies indicate higher stability in the validation analysis. N, the number of occurrences in the validations

level functions such as planning of future actions (Bludau et al. 2014), suppression and maintenance of internally-generated thoughts (Burgess et al. 2003), abstract information encoding (Bechara and Damasio 2005), and even being preferentially activated by episodic memory (Bludau et al. 2014). Neuroanatomical and functional connectivity studies also indicated that human FP receives a wide of projection from the OFC, amygdala, DLPFC, vmPFC, ACC, and PCC (Liu et al. 2013), suggesting a possible pattern of information communication and function integration in this region. Our previous studies also observed that FP represents the magnitude of delayed reward during inter-temporal choices (Wang et al. 2014a), and its gray matter volume (GMV) and regional homogeneity (ReHo) likewise is able to predict individual discounting behavior (Lv et al. 2019; Wang et al. 2016). Furthermore, the delay-discounting rates were significantly associated with the functional coupling of this seed with a series of brain areas, including vmPFC, VS, DLPFC, OP, and LOC (Wang et al. 2016). These studies, along with our present findings, suggest that FP not only engages to value representation but also is involved in higher-level integrated processing in inter-temporal decision-making.

Beyond the prefrontal system, limbic system is composed of the hippocampus, parahippocampus, amygdala, OFC, and ACC, which also play a crucial role in the delay-discounting. In particular, a number of neuroimaging studies have shown that hippocampus is able to up-modulate neural valuation signal in the ACC in order to decrease individual preferences for immediate rewards (Peters and Büchel 2010), especially via imagining in unfamiliar conditions (Sasse et al. 2015), and the white-matter integrity of this area (i.e., parahippocampus) was significantly correlated with the delay-discounting rates (Yu 2012). Also, existing studies have observed that the activation pattern of the limbic system (i.e., parahippocampus) can predict individuals' inter-temporal decisions (Chen et al. 2019a). In addition, increased activations in this system, especially for mOFC and putamen, reduced impulsive decisions (McClure et al. 2007; McClure et al. 2004), while lesions to this system were associated with steeper delay-discounting (Mariano et al. 2009; Mobini et al. 2002; Sellitto et al. 2010). Furthermore, neuroanatomical evidence of the limbic system, especially for the orbitofrontal cortex, reveals that this system receives information from the ventral or object processing visual stream, and taste, olfactory, and somatosensory inputs (Rolls 2004), which suggests the involvement of this system in sensory integration including affective value of reinforcers (Kringelbach 2005). Together with our present findings, these studies provide consistent evidence that global information communication/integration in the limbic system is crucial for individuals' inter-temporal decisions.

Connectome-based studies point out that brain regions with high FCS during the state of spontaneous neuronal activity might reflect the possibly high-effective information communication with other brain regions, which might support the possibility of information transfer during the task state. One possible interpretation is that these regions, also namely as "hubs" in brain network, frequently occupy a pivotal position in the communication and integration of the network to support various mental processes across a broad range of cognitive tasks, manifesting as increased regional cerebral blood flow as the cognitive demand (Cole et al. 2013; Liang et al. 2013; van den Heuvel and Sporns 2013). The structural hubs involve the precuneus, insula, superior parietal cortex, and superior frontal cortex via structural network analysis (Iturria-Medina et al. 2008), whereas the functional hubs are predominantly located in the ventral and dorsal precuneus, posterior and anterior cingulate gyrus, ventromedial frontal cortex, and inferior parietal brain regions (Tomasi and Volkow 2010; Zuo et al. 2011). Unexpectedly, network nodal connectivity capacity in hub brain regions was not observed predictive of individuals' inter-temporal decision-making in our present study, which is consistent with previous findings of no significant correlations between degree/betweenness centrality and delay-discounting rates (Chen et al. 2019b). These findings suggest that in a typical population, only solely hub region with higher global communication could not capture all characteristics of inter-temporal decisions because rich-club organization embedded in brain network's infrastructure was observed associated with discounting behavior (Chen et al. 2019b).

In addition to the all-range connectivity, both short- and long-distance functional connectivity also exhibited similar prediction on delay-discounting, which suggest that local and global communication with other brain regions support the implementation of inter-temporal choices. Disruption in local and global functional connectivity has been frequently observed in several psychiatric diseases such as AD/MCI (Liu et al. 2014), autism (Shukla et al. 2011), and even brain tumor patients (Douw et al. 2008), which imply that disconnection of brain regions is a possible reason explaining the underlying mechanisms of some brain diseases. Indeed, the present findings showed a negative correlation between short/long-distance FCS and discounting behavior, manifesting modulation decreases from hub regions possibly. To our knowledge, this is first work to systematically examine distance-based functional connectivity on inter-temporal decision-making, and further support the notion that parallel information processing is the most critical characteristics of human brain topological organization and changes in this metric are likely to manifest as dysfunction on cognitive processes such as decision-making, and even as a disease.

One particular region's long-distance connections (but not its short-distance connections) found in present study was the dorsomedial prefrontal cortex (DMPFC), which has been found by previous studies to play an influential role in inter-temporal choices (Wang et al. 2014a). Specifically, the anterior and posterior portions of DMPFC respectively represent delayed rewards and immediate rewards, and the value representation signals from these two subregions are relayed to the ventral striatum and ventromedial prefrontal cortex to compare value magnitude between two options during inter-temporal choice (Wang et al. 2014a). Moreover, morphological characteristics and functional organization of DMPFC (i.e., grey matter volume, regional homogeneity, and activation pattern during risky decision) have all been associated with discounting behaviors (Lv et al. 2019; Lv et al. 2020; Wang et al. 2016). Our study adds to these previous studies by emphasizing the role of long-distance interregional information communication of this target region in inter-temporal decision-making.

Several limitations of the current study need to be mentioned. First, this was a correlational study, so it could not provide definitive evidence for a causal relation between intrinsic brain functional connectivity in the limbic system and inter-temporal decision-making. Second, the functions of the relevant brain regions were inferred based on findings of the current and previous studies. Future research needs to investigate the specific functions and pathways of the limbic system including mOFC and parahippocampus with other brain regions**, especially using task-based fMRI design.** Moreover, future research is also needed to investigate the relationship between white matter fiber connectivity strength and delay-discounting in order to provide cross-validation of our results and to develop a comprehensive perspective for human decision impulsivity. Additionally, it is worth noting that 101 adolescents (age 17–18) were included in our analysis but no significant group differences between this group and adults group were observed in impulsivity scores ($t_{(427)} = 0.580$, $p = 0.494$) and in the functional connectivity strength. Such findings perhaps hint that neurodevelopment changes from adolescence to adulthood may do not influence our key conclusion of intrinsic non-hub connectivity important for inter-temporal decision-making.

Conclusions

Our study showed that intrinsic non-hub functional connectivity (i.e., mOFC and parahippocampus) could predict delay-discounting rates, and provided further support for the importance of distance-based functional connectivity, especially for DMPFC region, in the inter-temporal decision-making. These outcomes thus indicated this notion that the local and global parallel information communication capacity support the implementation of human high-level cognition such as decision-making.

Acknowledgments This work was supported by research grants from the Humanities and Social Science Fund Project of the Ministry of Education (20YJC190018), National Natural Science Foundation of China (31972906), and Entrepreneurship and Innovation Program for Chongqing Overseas Returned Scholars (cx2017049).

Compliance with ethical standards

Conflict of interest All authors declare no conflict of interest.

Ethical approval All procedures performed in studies involving human participants were in accordance with the ethical standards of the Institutional Review Board (IRB) of the Southwest University and Beijing Normal University.

Informed consent Informed consent was obtained from all participants or their parents included in the study.

References

Achard, S., Salvador, R., Whitcher, B., Suckling, J., & Bullmore, E. (2006). A resilient, low-frequency, small-world human brain functional network with highly connected association cortical hubs. *The Journal of Neuroscience, 16*(1), 63–72.

Alessi, S., & Petry, N. M. (2003). Pathological gambling severity is associated with impulsivity in a delay discounting procedure. *Behavioural Processes, 64*(3), 345–354.

Beasley, T. M., Erickson, S., & Allison, D. B. (2009). Rank-based inverse normal transformations are increasingly used, but are they merited? *Behavior Genetics, 39*(5), 580–595.

Bechara, A., & Damasio, A. R. (2005). The somatic marker hypothesis: A neural theory of economic decision. *Games and Economic Behavior, 52*(2), 336–372.

Berns, G. S., Laibson, D., & Loewenstein, G. (2007). Intertemporal choice–toward an integrative framework. *Trends in Cognitive Sciences, 11*(11), 482–488.

Bickel, W. K., Odum, A. L., & Madden, G. J. (1999). Impulsivity and cigarette smoking: Delay discounting in current, never, and ex-smokers. *Psychopharmacology, 146*(4), 447–454.

Bludau, S., Eickhoff, S. B., Mohlberg, H., Caspers, S., Laird, A. R., Fox, P. T., Schleicher, A., Zilles, K., & Amunts, K. (2014). Cytoarchitecture, probability maps and functions of the human frontal pole. *Neuroimage, 93*, 260–275.

Bondy, J. A., & Murty, U. S. R. (1976). *Graph theory with applications* (Vol. 290): Macmillan London.

Buckner, R. L., Sepulcre, J., Talukdar, T., Krienen, F. M., Liu, H., Hedden, T., Andrews-Hanna, J. R., Sperling, R. A., & Johnson, K. A. (2009). Cortical hubs revealed by intrinsic functional connectivity: Mapping, assessment of stability, and relation to Alzheimer's disease. *Journal of Neuroscience, 29*(6), 1860–1873.

Bullmore, E., & Sporns, O. (2009). Complex brain networks: Graph theoretical analysis of structural and functional systems. *Nature Reviews Neuroscience, 10*(3), 186–198.

Burgess, P. W., Scott, S. K., & Frith, C. D. (2003). The role of the rostral frontal cortex (area 10) in prospective memory: A lateral versus medial dissociation. *Neuropsychologia, 41*(8), 906–918.

Cai, H., Chen, J., Liu, S., Zhu, J., & Yu, Y. (2020). Brain functional connectome-based prediction of individual decision impulsivity. *cortex, 125*, 288–298.

Chen, Z., Guo, Y., & Feng, T. (2017). Delay discounting is predicted by scale-free dynamics of default mode network and salience network. *Neuroscience, 362*, 219–227.

Chen, Z., Guo, Y., Zhang, S., & Feng, T. (2019a). Pattern classification differentiates decision of intertemporal choices using multi-voxel pattern analysis. *cortex, 111*, 183–195.

Chen, Z., Hu, X., Chen, Q., & Feng, T. (2019b). Altered structural and functional brain network overall organization predict human intertemporal decision-making. *Human Brain Mapping, 40*(1), 306–328.

Clithero, J. A., Carter, R. M., & Huettel, S. A. (2009). Local pattern classification differentiates processes of economic valuation. *Neuroimage, 45*(4), 1329–1338.

Cole, M. W., Reynolds, J. R., Power, J. D., Repovs, G., Anticevic, A., & Braver, T. S. (2013). Multi-task connectivity reveals flexible hubs for adaptive task control. *Nature Neuroscience, 16*(9), 1348–1355.

Cox, D. D., & Savoy, R. L. (2003). Functional magnetic resonance imaging (fMRI) "brain reading": Detecting and classifying distributed patterns of fMRI activity in human visual cortex. *Neuroimage, 19*(2), 261–270.

Damoiseaux, J., Rombouts, S., Barkhof, F., Scheltens, P., Stam, C., Smith, S. M., et al. (2006). Consistent resting-state networks across healthy subjects. *Proceedings of the National Academy of Sciences, 103*(37), 13848–13853.

de Reus, M. A., & Van den Heuvel, M. P. (2013). The parcellation-based connectome: Limitations and extensions. *Neuroimage, 80*, 397–404.

Dombrovski, A. Y., Siegle, G. J., Szanto, K., Clark, L., Reynolds, C., & Aizenstein, H. (2012). The temptation of suicide: Striatal gray matter, discounting of delayed rewards, and suicide attempts in late-life depression. *Psychological Medicine, 42*(6), 1203–1215.

Douw, L., Baayen, H., Bosma, I., Klein, M., Vandertop, P., Heimans, J., Stam, K., de Munck, J., & Reijneveld, J. (2008). Treatment-related changes in functional connectivity in brain tumor patients: A magnetoencephalography study. *Experimental Neurology, 212*(2), 285–290.

Drucker, H., Burges, C. J., Kaufman, L., Smola, A. J., & Vapnik, V. (1997). Support vector regression machines*.* Paper presented at the Advances in neural information processing systems.

Eklund, A., Nichols, T. E., & Knutsson, H. (2016). Cluster failure: why fMRI inferences for spatial extent have inflated false-positive rates. *Proceedings of the National Academy of Sciences*, 201602413.

Fox, M. D., Snyder, A. Z., Vincent, J. L., Corbetta, M., Van Essen, D. C., & Raichle, M. E. (2005). The human brain is intrinsically organized into dynamic, anticorrelated functional networks. *Proceedings of the National Academy of Sciences, 102*(27), 9673–9678.

Franzmeier, N., Düzel, E., Jessen, F., Buerger, K., Levin, J., Duering, M., Dichgans, M., Haass, C., Suárez-Calvet, M., Fagan, A. M., Paumier, K., Benzinger, T., Masters, C. L., Morris, J. C., Perneczky, R., Janowitz, D., Catak, C., Wolfsgruber, S., Wagner, M., Teipel, S., Kilimann, I., Ramirez, A., Rossor, M., Jucker, M., Chhatwal, J., Spottke, A., Boecker, H., Brosseron, F., Falkai, P., Fliessbach, K., Heneka, M. T., Laske, C., Nestor, P., Peters, O., Fuentes, M., Menne, F., Priller, J., Spruth, E. J., Franke, C., Schneider, A., Kofler, B., Westerteicher, C., Speck, O., Wiltfang, J., Bartels, C., Araque Caballero, M. Á., Metzger, C., Bittner, D., Weiner, M., Lee, J. H., Salloway, S., Danek, A., Goate, A., Schofield, P. R., Bateman, R. J., & Ewers, M. (2018). Left frontal hub connectivity delays cognitive impairment in autosomal-dominant and sporadic Alzheimer's disease. *Brain, 141*(4), 1186–1200.

Freeman, L. C., Borgatti, S. P., & White, D. R. (1991). Centrality in valued graphs: A measure of betweenness based on network flow. *Social Networks, 13*(2), 141–154.

Hagmann, P., Cammoun, L., Gigandet, X., Meuli, R., Honey, C. J., Wedeen, V. J., & Sporns, O. (2008). Mapping the structural core of human cerebral cortex. *PLoS Biology, 6*(7), e159.

Haxby, J. V. (2012). Multivariate pattern analysis of fMRI: The early beginnings. *Neuroimage, 62*(2), 852–855.

Haxby, J. V., Connolly, A. C., & Guntupalli, J. S. (2014). Decoding neural representational spaces using multivariate pattern analysis. *Annual Review of Neuroscience, 37*, 435–456.

He, Q., Xue, G., Chen, C., Chen, C., Lu, Z.-L., & Dong, Q. (2013). Decoding the neuroanatomical basis of reading ability: A multivoxel morphometric study. *Journal of Neuroscience, 33*(31), 12835–12843.

He, Y., Chen, Z., & Evans, A. (2007). Small-world anatomical networks in the human brain revealed by cortical thickness from MRI. *Cerebral Cortex, 17*(10), 2407–2419.

Hu, S., Ide, J. S., Zhang, S., Sinha, R., & Chiang-shan, R. L. (2015). Conflict anticipation in alcohol dependence—A model-based fMRI study of stop signal task. *Neuroimage: Clinical, 8*, 39–50.

Iturria-Medina, Y., Sotero, R. C., Canales-Rodríguez, E. J., Alemán-Gómez, Y., & Melie-García, L. (2008). Studying the human brain anatomical network via diffusion-weighted MRI and graph theory. *Neuroimage, 40*(3), 1064–1076.

Jimura, K., & Poldrack, R. A. (2012). Analyses of regional-average activation and multivoxel pattern information tell complementary stories. *Neuropsychologia, 50*(4), 544–552.

Johnson, M. W., & Bickel, W. K. (2002). Within-subject comparison of real and hypothetical money rewards in delay discounting. *Journal of the Experimental Analysis of Behavior, 77*(2), 129–146.

Kriegeskorte, N., Goebel, R., & Bandettini, P. (2006). Information-based functional brain mapping. *Proceedings of the National Academy of Sciences, 103*(10), 3863–3868.

Kringelbach, M. L. (2005). The human orbitofrontal cortex: Linking reward to hedonic experience. *Nature Reviews Neuroscience, 6*(9), 691–702.

Lempert, K. M., & Phelps, E. A. (2016). The malleability of intertemporal choice. *Trends in Cognitive Sciences, 20*(1), 64–74.

Li, N., Ma, N., Liu, Y., He, X.-S., Sun, D.-L., Fu, X.-M., Zhang, X., Han, S., & Zhang, D. R. (2013). Resting-state functional connectivity predicts impulsivity in economic decision-making. *Journal of Neuroscience, 33*(11), 4886–4895.

Liang, X., Zou, Q., He, Y., & Yang, Y. (2013). Coupling of functional connectivity and regional cerebral blood flow reveals a physiological basis for network hubs of the human brain. *Proceedings of the National Academy of Sciences, 110*(5), 1929–1934.

Liu, H., Qin, W., Li, W., Fan, L., Wang, J., Jiang, T., & Yu, C. (2013). Connectivity-based parcellation of the human frontal pole with diffusion tensor imaging. *Journal of Neuroscience, 33*(16), 6782–6790.

Liu, J., Xia, M., Dai, Z., Wang, X., Liao, X., Bi, Y., et al. (2017). Intrinsic brain hub connectivity underlies individual differences in spatial working memory. *Cerebral Cortex, 27*(12), 5496–5508.

Liu, Y., Yu, C., Zhang, X., Liu, J., Duan, Y., Alexander-Bloch, A. F., Liu, B., Jiang, T., & Bullmore, E. (2014). Impaired long distance functional connectivity and weighted network architecture in Alzheimer's disease. *Cerebral Cortex, 24*(6), 1422–1435.

Lv, C., Wang, Q., Chen, C., Qiu, J., Xue, G., & He, Q. (2019). The regional homogeneity patterns of the dorsal medial prefrontal cortex predict individual differences in decision impulsivity. *Neuroimage, 200*, 556–561.

Lv, C., Wang, Q., Chen, C., Xue, G., & He, Q. (2020). Activation patterns of the dorsal medial prefrontal cortex and frontal pole predict individual differences in decision impulsivity. *Brain Imaging and Behavior In press*.

Mariano, T., Bannerman, D., McHugh, S., Preston, T., Rudebeck, P., Rudebeck, S., et al. (2009). Impulsive choice in hippocampal but not orbitofrontal cortex-lesioned rats on a nonspatial decision-making maze task. *European Journal of Neuroscience, 30*(3), 472–484.

McClure, S. M., Ericson, K. M., Laibson, D. I., Loewenstein, G., & Cohen, J. D. (2007). Time discounting for primary rewards. *Journal of Neuroscience, 27*(21), 5796–5804.

McClure, S. M., Laibson, D. I., Loewenstein, G., & Cohen, J. D. (2004). Separate neural systems value immediate and delayed monetary rewards. *Science, 306*(5695), 503–507.

McNamee, D., Rangel, A., & O'doherty, J. P. (2013). Category-dependent and category-independent goal-value codes in human ventromedial prefrontal cortex. *Nature Neuroscience, 16*(4), 479–485.

Mobini, S., Body, S., Ho, M.-Y., Bradshaw, C., Szabadi, E., Deakin, J., & Anderson, I. M. (2002). Effects of lesions of the orbitofrontal cortex on sensitivity to delayed and probabilistic reinforcement. *Psychopharmacology, 160*(3), 290–298.

Norman, K. A., Polyn, S. M., Detre, G. J., & Haxby, J. V. (2006). Beyond mind-reading: Multi-voxel pattern analysis of fMRI data. *Trends in Cognitive Sciences, 10*(9), 424–430.

Oldham, S., & Fornito, A. (2019). The development of brain network hubs. *Developmental Cognitive Neuroscience, 36*, 100607.

Öngür, D., Ferry, A. T., & Price, J. L. (2003). Architectonic subdivision of the human orbital and medial prefrontal cortex. *Journal of Comparative Neurology, 460*(3), 425–449.

Paloyelis, Y., Asherson, P., Mehta, M. A., Faraone, S. V., & Kuntsi, J. (2010). DAT1 and COMT effects on delay discounting and trait impulsivity in male adolescents with attention deficit/hyperactivity disorder and healthy controls. *Neuropsychopharmacology, 35*(12), 2414–2426.

Peters, J., & Büchel, C. (2010). Episodic future thinking reduces reward delay discounting through an enhancement of prefrontal-mediotemporal interactions. *Neuron, 66*(1), 138–148.

Peters, J., & Büchel, C. (2011). The neural mechanisms of inter-temporal decision-making: Understanding variability. *Trends in Cognitive Sciences, 15*(5), 227–239.

Ramnani, N., & Owen, A. M. (2004). Anterior prefrontal cortex: Insights into function from anatomy and neuroimaging. *Nature Reviews Neuroscience, 5*(3), 184–194.

Rolls, E. T. (2004). The functions of the orbitofrontal cortex. *Brain and Cognition, 55*(1), 11–29.

Sasse, L. K., Peters, J., Büchel, C., & Brassen, S. (2015). Effects of prospective thinking on intertemporal choice: The role of familiarity. *Human Brain Mapping, 36*(10), 4210–4221.

Sellitto, M., Ciaramelli, E., & di Pellegrino, G. (2010). Myopic discounting of future rewards after medial orbitofrontal damage in humans. *Journal of Neuroscience, 30*(49), 16429–16436.

Shin, D.-J., Jung, W. H., He, Y., Wang, J., Shim, G., Byun, M. S., Jang, J. H., Kim, S. N., Lee, T. Y., Park, H. Y., & Kwon, J. S. (2014). The effects of pharmacological treatment on functional brain connectome in obsessive-compulsive disorder. *Biological Psychiatry, 75*(8), 606–614.

Shukla, D. K., Keehn, B., Smylie, D. M., & Müller, R.-A. (2011). Microstructural abnormalities of short-distance white matter tracts in autism spectrum disorder. *Neuropsychologia, 49*(5), 1378–1382.

Sporns, O. (2011). The human connectome: A complex network. *Annals of the New York Academy of Sciences, 1224*(1), 109–125.

Sporns, O., Honey, C. J., & Kotter, R. (2007). Identification and classification of hubs in brain networks. *PLoS One, 2*(10), e1049.

Tomasi, D., & Volkow, N. D. (2010). Functional connectivity density mapping. *Proceedings of the National Academy of Sciences, 107*(21), 9885–9890.

van den Bos, W., Rodriguez, C. A., Schweitzer, J. B., & McClure, S. M. (2014). Connectivity strength of dissociable striatal tracts predict individual differences in temporal discounting. *Journal of Neuroscience, 34*(31), 10298–10310.

Van Den Bos, W., Rodriguez, C. A., Schweitzer, J. B., & McClure, S. M. (2015a). Adolescent impatience decreases with increased frontostriatal connectivity. *Proceedings of the National Academy of Sciences, 112*(29), E3765–E3774.

Van Den Bos, W., Rodriguez, C. A., Schweitzer, J. B., & McClure, S. M. (2015b). Adolescent impatience decreases with increased frontostriatal connectivity. *Proceedings of the National Academy of Sciences*, 201423095.

van den Heuvel, M. P., & Sporns, O. (2013). Network hubs in the human brain. *Trends in Cognitive Sciences, 17*(12), 683–696.

Wang, Q., Chen, C., Cai, Y., Li, S., Zhao, X., Zheng, L., Zhang, H., Liu, J., Chen, C., & Xue, G. (2016). Dissociated neural substrates underlying impulsive choice and impulsive action. *Neuroimage, 134*, 540–549.

Wang, Q., Luo, S., Monterosso, J., Zhang, J., Fang, X., Dong, Q., & Xue, G. (2014a). Distributed value representation in the medial prefrontal cortex during intertemporal choices. *Journal of Neuroscience, 34*(22), 7522–7530.

Wang, X., Xia, M., Lai, Y., Dai, Z., Guo, Q., Cheng, Z., et al. (2014b). Disrupted resting-state functional connectivity in minimally treated chronic shiziphrenia. *Schizophrenia Research, 156*(2014), 150–156.

Yu, R. (2012). Regional white matter volumes correlate with delay discounting. *PLoS One, 7*(2), e32595.

Zha, R., Bu, J., Wei, Z., Han, L., Zhang, P., Ren, J., Li, J. A., Wang, Y., Yang, L., Vollstädt-Klein, S., & Zhang, X. (2019). Transforming brain signals related to value evaluation and self-control into behavioral choices. *Human Brain Mapping, 40*(4), 1049–1061.

Zhang, W., Li, S., Wang, X., Gong, Y., Yao, L., Xiao, Y., Liu, J., Keedy, S. K., Gong, Q., Sweeney, J. A., & Lui, S. (2018). Abnormal dynamic functional connectivity between speech and auditory areas in schizophrenia patients with auditory hallucinations. *Neuroimage: Clinical, 19*, 918–924.

Zuo, X.-N., Ehmke, R., Mennes, M., Imperati, D., Castellanos, F. X., Sporns, O., & Milham, M. P. (2011). Network centrality in the human functional connectome. *Cerebral Cortex, 22*(8), 1862–1875.